

# Comparative proteomic analysis of kinesin-8B deficient Plasmodium berghei during gametogenesis

Carlos Henrique Saraiva Garcia, Delphine Depoix, Paulo Costa Carvalho, Izabela Marques Dourado Bastos, Carlos André Ornelas Ricart, Marcelo Valle de Sousa, David J.P. Ferguson, Jaime Martins Santana, Philippe Grellier, Sébastien Charneau

▶ **To cite this version:**

Carlos Henrique Saraiva Garcia, Delphine Depoix, Paulo Costa Carvalho, Izabela Marques Dourado Bastos, Carlos André Ornelas Ricart, et al.. Comparative proteomic analysis of kinesin-8B deficient Plasmodium berghei during gametogenesis. Journal of Proteomics, 2021, 236, pp.104118. 10.1016/j.jprot.2021.104118 . mnhn-03221599

**HAL Id: mnhn-03221599**
**https://mnhn.hal.science/mnhn-03221599**

Submitted on 13 Feb 2023

**HAL** is a multi-disciplinary open access archive for the deposit and dissemination of scientific research documents, whether they are published or not. The documents may come from teaching and research institutions in France or abroad, or from public or private research centers.

L'archive ouverte pluridisciplinaire **HAL**, est destinée au dépôt et à la diffusion de documents scientifiques de niveau recherche, publiés ou non, émanant des établissements d'enseignement et de recherche français ou étrangers, des laboratoires publics ou privés.



Distributed under a Creative Commons Attribution - NonCommercial 4.0 International License

Version of Record: https://www.sciencedirect.com/science/article/pii/S1874391921000178
Manuscript_0d08a49c97a78ddd9c7a7d0ee66975a6

# Comparative proteomic analysis of kinesin-8B deficient *Plasmodium berghei* during gametogenesis

Carlos Henrique Saraiva Garcia[a,b], Delphine Depoix[b], Paulo Costa Carvalho[c], Izabela Marques Dourado Bastos[d], Carlos André Ornelas Ricart[a], Marcelo Valle de Sousa[a], David J. P. Ferguson[e], Jaime Martins Santana[d], Philippe Grellier[b,*] and Sébastien Charneau[a,*]

a Laboratory of Protein Chemistry and Biochemistry, Department of Cell Biology, Institute of Biology, University of Brasilia, Brasilia, 70910–900 Brazil.
b UMR 7245 Molécules de Communication et Adaptation des Micro-organismes, Muséum National d'Histoire Naturelle, CNRS, CP52, 61 rue Buffon, 75231 Paris Cedex 05, France.
c Laboratory for Structural and Computational Mass Spectrometry, Carlos Chagas Institute, Fiocruz, Parana, Brazil.
d Pathogen-Host Interface Laboratory, Department of Cell Biology, Institute of Biology, University of Brasilia, Brasilia, 70910–900 Brazil.
e Nuffield Department of Clinical Laboratory Science, University of Oxford, John Radcliffe Hospital, Oxford, UK and Department of Biological and Medical Sciences, Faculty of Health and Life Science, Oxford Brookes University, Oxford, UK.

**Corresponding Authors**

* Tel : +33(0)140793510, e-mail : philippe.grellier@mnhn.fr (Philippe Grellier, PhD); Tel : +556131073127, e-mail : charneau@unb.br (Sébastien Charneau, PhD).

© 2021 published by Elsevier. This manuscript is made available under the CC BY NC user license
https://creativecommons.org/licenses/by-nc/4.0/

**KEYWORDS:**
*Plasmodium*, gametogenesis, exflagellation, quantitative proteomics, kinesin, mutant

**ABSTRACT**

*Plasmodium* blood stages, responsible for human to vector transmission, termed gametocytes, are the precursor cells that develop into gametes in the mosquito. Male gametogenesis works as a bottleneck for the parasite life cycle, where, during a peculiar and rapid exflagellation, a male gametocyte produces 8 intracellular axonemes that generate by budding 8 motile gametes. Understanding the molecular mechanisms of gametogenesis is key to design strategies for controlling malaria transmission. In the rodent *P. berghei*, the microtubule-based motor kinesin-8B (PbKIN8B) is essential for flagellum assembly during male gametogenesis and its gene disruption impacts on completion of the parasitic life cycle. In efforts to improve our knowledge about male gametogenesis, we performed an iTRAQ-based quantitative proteomic comparison of *P. berghei* mutants with disrupted *kinesin-8B* gene (Δ*Pbkin8B*) and wild type parasites. During the 15 min of gametogenesis, Δ*Pbkin8B* parasites exhibited important motor protein dysregulation that suggests an essential role of PbKIN8B for the correct interaction or integration of axonemal proteins within the growing axoneme. The energy metabolism of Δ*Pbkin8B* mutants was further affected, as well as the response to stress proteins, protein synthesis, as well as chromatin organisation and DNA processes, although endomitoses seemed to occur.

***Significance:***

Malaria continues to be a global scourge, mainly in subtropical and tropical areas. The disease is caused by parasites from the *Plasmodium* genus. *Plasmodium* life cycle alternates between female *Anopheles* mosquitoes and vertebrate hosts through bites. Gametocytes are the parasite blood forms responsible for transmission from vertebrates to vectors. Inside the mosquito midgut, after stimulation, male and female gametocytes transform into gametes resulting in fertilization. During male gametogenesis, one gametocyte generates eight intracytoplasmic axonemes that generate, by budding, flagellated motile gametes involving a process termed exflagellation. Sexual development has a central role in ensuring malaria transmission. However, molecular data on male gametogenesis and particularly on intracytoplasmic axoneme assembly are still lacking. Since rodent malaria parasites permit the

combination of *in vivo* and *in vitro* experiments and reverse genetic studies, our group investigated the molecular events in rodent *P. berghei* gametogenesis. The *P. berghei* motor ATPase kinesin-8B is proposed as an important component for male gametogenesis. We generated *Pbkin*8B gene-disrupted gametocytes (Δ*Pbkin8B*) that were morphologically similar to the wild- type (WT) parasites. However, in mutants, male gametogenesis is impaired, male gametocytes are disabled in their ability to assemble axonemes and to exflagellate to release gametes, reducing fertilization drastically. Using a comparative quantitative proteomic analysis, we associated the nonfunctional axoneme of the mutants with the abnormal differential expression of proteins essential to axoneme organization and stability. We also observed a differential dysregulation of proteins involved in protein biosynthesis and degradation, chromatin organisation and DNA processes in Δ*Pbkin8B* parasites, although DNA condensation, mitotic spindle formation and endomitoses seem to occur. This is the first functional proteomic study of a kinesin gene-disrupted *Plasmodium* parasite providing new insights into *Plasmodium* male gametogenesis.

## 1. INTRODUCTION

Malaria is one of the most serious human parasitic diseases, endemic mainly in subtropical and tropical areas, and continues to kill more than 400,000 people each year [1]. Many pharmacotherapy strategies and vaccine approaches have focused on the asexual parasite stages affecting humans, in most cases to mitigate the symptoms of disease [2]. On the other hand, *Plasmodium spp.* sexual development and propagation from vertebrate hosts to the mosquitos has attracted attention in the scientific community [3-6] as a means of interrupting the parasite life cycle and consequently parasite transmission.

*Plasmodium spp.* sexual development is dependent on the function and regulation of a set of motor proteins [7], that, when perturbed, can significantly affect the parasite's life cycle and its transmission [5]. This holds true especially for the *Plasmodium* male gamete that is the only developmental stage that possesses a flagellum. There are three core motor protein superfamilies encoded by most organisms: myosins, kinesins, and dyneins [8, 9]. Among these, kinesins are largely found in eukaryotes [9] and play important structural and functional roles in cilia and flagella [10], as well as mitosis [7]. Kinesins are motor enzymes that interact with microtubules and most use ATP-hydrolysis energy to move along microtubules, bringing with them cellular vesicles [11, 12], organelles or chromosomes [13]. They have further cellular tasks in morphology shaping, organelle segregation and microtubule regulation [14, 15], as well as a probable role in distal flagella assembly in eukaryotes [10, 16].

Currently, kinesins are classified in 14 families, called kinesin-1 to 14, according to the conserved motor domain [17] that does not necessarily share the same function among different organisms [18]**,** with the exception of the kinesin-5 family involved in the activity of mitotic spindles in plants and animals [18]. Furthermore, kinesin variants can participate in a manifold of responses and have various end uses in the eukaryotic cells [9, 12, 14, 15, 19, 20]. For example, kinesins are important for essential processes within the spermatogenesis of *Marsilea vestita* [18] and for normal flagellar function in *Chlamydomonas* [10].

Only 10 kinesin encoding genes can be found in the genome of the rodent malaria parasite *P. berghei* ANKA strain (plasmodb.org). Three of them have been identified by proteomic studies in male gametocytes and gametes. They belong to the families kinesin-8 (subfamily 8B), -13 and -15 [21-23], and are phosphoregulated during *P. berghei* gametocyte activation [24]. Male gametogenesis of *P. berghei* is a rapid process occurring within 15-20 min which involves 1) xanthurenic acid-triggered calcium signalling to activate $Ca^{2+}$-dependent protein kinases; 2) egress of the parasites from the red blood cells (RBCs) by lysis

of the parasitophorous vacuole and the erythrocyte membranes; 3) three rounds of rapid mitotic DNA replication associated with the intracytoplasmic assembly of 8 axonemes resulting in the production of 8 highly motile male gametes from a single parental gametocyte, that detach from the residual body by a process called exflagellation [25].

To improve our knowledge about male gamete morphogenesis and exflagellation, we focused on the study of kinesin-8B (PbKIN8B; PBANKA_0202700), initially identified as *Plasmodium* male gamete-specific [22]. In eukaryotic cells, kinesin-8 members migrate towards the microtubule plus-end terminus, according to its length [19], and accumulates there [19, 20]. Kinesin-8 family could act on microtubule rescue or catastrophic events that regulate the microtubule dynamicity [14, 15]. *Pbkin8B*-disrupted *P. berghei* gametocytes (Δ*Pbkin8B*) were produced and their phenotype studied [26, 27]. Δ*Pbkin8B* male and female gametocytes were morphologically and quantitatively similar to wild-type (WT) parasites. Mutant female gametes develop normally, whereas, in contrast, mutant male gametogenesis was severely impaired. Genome replication occurs, but male gamete axoneme formation and release were aborted. Analysis of Δ*Pbkin8B* male gametocytes ultrastructure revealed a default in axoneme assembly: elongated microtubules were seen in longitudinal sections but the classical 9+2 axoneme organisation was not observed [26, 27]. A dynamic cytoplasmic localisation of PbKIN8B with the basal bodies and the assembling axoneme was observed, indicating an essential role of PbKIN8B in parasite flagellum formation [27].

We performed relative protein quantitative comparisons during the xanthurenic acid induced-gametogenesis of the WT and Δ*Pbkin8B* parasite *P. berghei* using iTRAQ labelled peptides to better understand the molecular mechanisms underlying the ontogenetic formation of *Plasmodium* gametes. Time-course analyses were carried out for 7 and 15 min after gametogenesis induction. In WT parasites, from 2,617 iTRAQ-labelled peptides, 49 proteins were found differentially abundant during gametogenesis [21]. In the present study, we present the iTRAQ-based quantitative and comparative proteomic analysis of Δ*Pbkin8B* line against the previous WT *P. berghei* analysis, performed in parallel during the time-course of the xanthurenic acid-induced gamete development.

## 2. MATERIAL AND METHODS

### 2.1. Ethical compliance

All the experiments using rodents in this study were carried out according to European regulations in compliance with the French guidelines and regulations and approved by the Ethic Committee CUVIER (authorization n°68-007).

### 2.2. Parasites

A pyrimethamine-sensitive clone of *P. berghei* NK65 strain (kindly provided by R. Ménard, Pasteur Institute, Paris, France) was used throughout this study to infect mice as described by Janse and collaborators [28].

### 2.3. Generation of Δ*Pbkin8B* parasites

#### 2.3.1. *Plasmid for gene disruption*

For disruption of the *kinesin-8B* gene (PBANKA_0202700) by insertion, an internal gene sequence was amplified by polymerase chain reaction (PCR) using genomic DNA from the *P. berghei* NK65 strain and oligonucleotides forward 109 (5'-GGAATTCGAAGGAACCGAACTATTAAATG-3') and reverse 110 (5'-TCCCCGCGGCTGCACCAGTAGCTCCATATG-3') (*Eco*RI and *Sac*II sites respectively are underlined) and cloned into the vector b3D.DT^H.^D(pL0001) (Janse and collaborators) supplied by the Malaria Research and Reference Reagent Resource Center; MR4/ATCC (Manassas, VA, USA). Recombinant plasmid was linearized by *Xba*I digestion (nt 544 of the 1164 bp insert) (Suppl. Fig. 1A).

#### 2.3.2. *Parasite transfection and selection of Δ*Pbkin8B mutants*

*P. berghei* transfection was performed as previously described [29]. Briefly, after overnight culture (37 °C, 5% $CO_2$) of infected blood, mature schizonts were purified using a 55% Nycodenz gradient and collected at room temperature (RT). The mix for electroporation was composed of 10 µL of parasites (containing about $10^7$ mature schizonts), 100 µL of 88A6 Nucleofector solution (Lonza, Europe) and 10 µL of TE buffer containing 8 µg of digested plasmid DNA. Electroporation was performed using the U33 program of the nucleofector™ electroporator (Lonza, Europe), and electroporated parasites were resuspended in RPMI medium and injected immediately intravenously into 3-weeks-old female Swiss OF1 mice.

Recipient mice were treated with pyrimethamine in drinking water (0.07 mg/mL), starting 24 h post-infection. Pyrimethamine-resistant parasites were subsequently cloned by limiting dilution. Transfection experiments for gene disruption strategy were carried out twice on different days using different batches of material. Following drug selection, two independent clonal populations of Δ*Pbkin8B* mutant were selected by limiting dilution. Their genotype was validated by PCR (Suppl. Fig. 1B).

### 2.4. *In vivo Plasmodium berghei* gametocyte production and *in vitro* gamete exflagellation assay

*P. berghei* was maintained by cyclic passage in 4-6 week old female Swiss OF1 (Janvier, Le Genest Saint Isle, France). Enrichment and purification of gametocytes were achieved using a modified protocol from [30], as described in [31]. Briefly, mice were treated Intraperitoneally (IP) with 100 µL of 25 mg/mL phenylhydrazine in saline solution to induce hyper-reticulocytosis [32]. Two to three days later, mice were inoculated IP with $10^7$ infected RBCs from a donor mouse. At day 3 post-infection, mice were treated with sulfadiazine (Sigma) at 15 mg/L in drinking water for two days to kill asexual blood stages [21]. On day five post-infection, parasites were mainly constituted of gametocyte stages. Mice were euthanized and blood was harvested with heparin and kept on ice to avoid premature gametocyte activation. Gametocytes-infected RBCs were separated from uninfected erythrocytes by a 48% Nycodenz gradient (27.6% w/v Nycodenz in 5 mM Tris-HCl, pH 7.2, 3 mM KCl, 0.3 mM EDTA) in coelenterazine loading buffer (CLB: containing PBS, 20 mM HEPES, 20 mM Glucose, 4 mM sodium bicarbonate, 1 mM EDTA, 0.1% w/v bovine serum albumin, pH 7.25) during 10 min at 1,000 x g. Gametocyte-infected RBCs were collected at the interphase, transferred into CLB-containing tubes, centrifuged 1 min at 800 x g. The gametogenesis of the purified infected erythrocytes was immediately activated by addition of xanthurenic acid (XA, 100 µM final concentration) and directly fixed at different times post induction for microscopy assays. For proteomics, the pellet was resuspended in CLB, for preparation of Giemsa-stained blood smears. One third of the sample was immediately frozen in nitrogen liquid (Time 0) and xanthurenic acid (100 µM final concentration) was immediately added to the remaining two thirds to activate male gamete gametogenesis at RT. A small amount of cell suspension was mounted onto a Malassez chamber to count the RBC number and to follow up the exflagellation process under microscope. Half of the activated sample was frozen in liquid nitrogen after 7 min and the remainder after 15 min. Samples

were stored at -80 °C. All samples were prepared in biological triplicates. Purity was determined with Giemsa-stained smears.

### 2.5. Immunofluorescence assays (IFA)

Infected erythrocytes were fixed at 2, 8, 12 and 15 min after XA induction of gametogenesis overnight in 3.7% (v/v) formaldehyde + 0.002% glutaraldehyde in PBS at 4 °C. After a wash in PBS, cells were sedimented on poly-L-lysine-coated slides and permeabilized in 0.5% (v/v) NP40 in PBS for 15 min. Slides were saturated in PBS-NP40-milk (0.01% (v/v) NP40, 5% (w/v) non-fat milk in PBS) 30 min then incubated for 2 h with the anti α-tubulin II (mouse TAT1 antibody) in PBS-NP40-milk (0.01% (v/v) NP40, 1% (w/v) non-fat milk in PBS). Slides were washed three times in PBS and incubated for 1 h with Alexa 488-conjugated anti-mouse antibodies. After three washes in PBS and a 5 min incubation with 5 µg/ml DAPI followed by a final wash. Slides were mounted in VECTASHIELD antifade mounting medium (Vector Laboratories) and viewed using a Nikon Eclipse TE 300 DV inverted microscope with a 100X oil objective mounted on a piezo electric device using appropriate fluorescence emission filters. Image acquisition (z-series) was performed with a back illuminated cooled detector (Photometrics CoolSnap HQ, 12 bits, RoperScientific, France) using a 0.25 µm step. Image processes were performed using Image J software (http://rsb.info.nih.gov/ij/). The images presented correspond to the maximum intensity projection of the z-series.

### 2.6. Electron microscopy

Purified gametocytes were fixed 15 min post induction in 2.5% glutaraldehyde in 0.1 M phosphate buffer and processed for electron microscopy using a JEOL1200EX electron microscope (Jeol UK Ltd) as previously described [26].

### 2.7. Sample preparation for LC-MS/MS

Each sample was lysed in 10 volumes of 8.0 M urea containing a complete mixture of protease and phosphatase inhibitors 2X (Halt Protease and Phosphatase Inhibitor Cocktail 100X, Thermo Scientific), through three rapid cycles of freezing in liquid nitrogen and thawing on ice. Lysates were lyophilized and stored at -80 °C until use. Lyophilized samples were resuspended in 100 mM TEAB (Fluka), vigorously vortexed and diluted with 4 volumes

of ice-cold ethanol. After homogenization, 4 volumes of ice-cold acetone were added. Sample was vigorously vortexed and incubated overnight at -20 °C for protein precipitation. Sample was then centrifuged at 13,000 x g, 15 min, at 4 °C and the supernatant was discarded. The pellet was washed three times with ice-cold ethanol/acetone/water solution (4/4/2). Proteins were resolubilized in 8 M urea in 100 mM TEAB, centrifuged at 13,000 x g, 15 min, at 4 °C and the supernatant transferred into a new tube. Proteins were reduced by 20 mM DTT at RT for one hour and alkylated with 40 mM iodoacetamide for another hour. Proteins were first digested at RT by endoproteinase Lys-C (Sigma-Aldrich) for 12 h with 0.01 AU for 100 µg of proteins. The solution was then diluted with 100 mM TEAB and 10% acetonitrile to a final urea concentration of 1 M, supplemented with 1 µg of trypsin per 100 µg of proteins (Sequencing Grade Modified Trypsin, Promega), for 4 hr at RT. The peptide sample was acidified with 0.1% (v/v) TFA, final concentration, and desalted using homemade 2 cm long Poros 20 R2 and Oligo R3 (Applied Biosystems) microcolumns packed in p200 tips [33]. Peptides were eluted with 70% acetonitrile/0.1% TFA. Dried up samples were solubilized in 300 mM TEAB and peptide concentration was determined by Qubit® quantification assay (Thermo Fischer).

### 2.8. iTRAQ labelling

Samples were labelled by 4-plex iTRAQ Reagent Multi-plex Kit (Applied Biosystems) according to the manufacturer's instruction. The iTRAQ labelled-sample combinations were designed to allow separate analysis of the WT *P. berghei* and of the Δ*Pbkin8B* line in their respective biological and experimental replicates during the inducted gametogenesis as following: isotope 114: time 0, isotope 115: time 7 min, isotope 116: time 15 min for WT as previously reported [21] and isotope 117: time 0, isotope 114: time 7 min, isotope 115: time 15 min for Δ*Pbkin8B*, and finally multiplexing both lines. Labelling efficiency was controlled by micro-analysis by mass spectrometry for each labelled sample (1 µL). After normalization, labelled samples were mixed in equal proportion.

### 2.9. LC-MS/MS

Peptides were analysed in biological triplicate with two technical repetitions each using a Dionex Ultimate™ 3000 RSLCnano system (Thermo Fisher Scientific, Waltham, MA) coupled online with an LTQ-Orbitrap Elite™ mass spectrometer (Thermo Scientific,

San Jose, CA). Samples were first loaded onto a 200 µm x 100 µm fused silica emitter trap column in-house packed with Reprosil-Pur 120 Å C18-AQ 5 µm resin (Dr. Maisch GmbH, Ammerbuch, Germany) and then fractionated by 35 cm reverse phase capillary column made by fused silica emitter (75 µm inner diameter) packed in-house with Reprosil-Pur 120 Å C18-AQ 3 µm resin (Dr. Maisch GmbH, Ammerbuch, Germany). In brief, peptides in 0.1% (v/v) formic acid were injected onto the trap column with 98% solvent A (0.1% formic acid in water) and 2% solvent B (0.1% formic acid in acetonitrile) under flow rate of 3 µL/min. After washing, peptides were resolved over 210 minutes with 230 nL/min flow rate in analytical column through use of organic gradients: 2-40% solvent B until 170 min; and then 40-85% until 185 min; 85% until 190 min; and at least 2% until 210 min. Peptides were ionized by Nanospray Flex$^{TM}$ ion source (Thermo Fisher Scientific, Waltham, MA, USA) ionization at 2.5 kV and a capillary temperature of 275 °C.

### 2.10. Data processing

Data were acquired in a positive mode by Data-Dependent Acquisition (DDA) operated by the software Xcalibur 2.2 SP 1.78 (Thermo Fisher Scientific, CA, USA). DDA survey scans were set to 120.000 FWHM, m/z of 400, in the m/z range of 300 to 1800 and the top 15 multiply charged ions in each duty cycle selected for MS/MS fragmentation using higher-energy collisional dissociation (HCD) with a normalized collision energy of 50%, and 35% in technical replicate. The mass spectrometry data have been deposited to the ProteomeXchange Consortium (http://proteomecentral.proteomexchange.org) via the PRIDE partner repository [34] with the dataset identifiers PXD020892 and PXD020911.

### 2.11. Data analysis

PatternLab v.4.0.0.27 was used for identification and quantitative comparison of proteins (http://www.patternlabforproteomics.org). The search was done using Comet which is embedded into PatternLab. The database used was a combination of 5,143 protein sequences of *Plasmodium berghei* ANKA downloaded from PlasmoDB, 55,957 sequences of *Mus musculus* downloaded from NCBInr plus 127 common contaminants to mass spectrometry automatically included by Patternlab. The .raw files were searched according to the following parameters: semi-tryptic and tryptic peptides hydrolytic enzyme specificity,

tolerance of two missed cleavages, cabamidomethylation of cysteines and N-terminus iTRAQ-4plex tagging of lysine residues as fixed modification, iTRAQ-4plex in tyrosine as variable modification, Fragment bin tolerance of 0.02, MS/MS and precursor tolerance of 40 ppm, the search mass range was of 550 to 5,500 Da. We then used PatternLab's SEPro to converge to a final list of confident identifications satisfying a 1% FDR at the protein level as per bioinformatics protocol [35]; identifications with more than 10 ppm at the precursor lever were also discarded. The PSM results from all replicates were mapped to protein groups. Our quantitative analysis only considered proteins with two or more unique peptides and peptides with fold changes greater than 20% and p-value < 0.05.

### 2.12. Gene Ontology

The functional categorization of proteins was assessed using Blast2GO software v.3.3.0 (Oracle Corporation). The primary sequence of each protein identified by PSM was exported from PatternLab in FASTA format and blasted by Blast2GO using default parameters with exception of Word Size of 3 and number of hits increased to 30. All alignments were carried out using BlastP v2.2.31+ service from CloundBlast (BioBam Bioinformatics S.L. Valencia, Spain) and all organisms in the NCBInr database.

## 3. RESULTS

### 3.1. Δ*Pbkin8B* mutant phenotype

We generated transgenic parasites where the *kinesin-8B* gene was disrupted (Suppl. Fig. 1), which was named Δ*Pbkin8B*. Examination of the parasite life cycle showed normal intraerythrocytic development confirming that the endogenous gene is nonessential for parasite growth. In contrast, male gametogenesis was strongly impaired in mutants compared to WT. Only a few exflagellation events were recorded in Δ*Pbkin8B* parasites compared to WT (Suppl. Fig. 2), confirming that kinesin-8B plays a crucial role in the completion of *P. berghei* male gametogenesis [26, 27]. IFAs performed during the course of male gametogenesis evidenced a reorganisation of α–tubulin II in WT and Δ*Pbkin8B* mutant to assemble microtubules in the cytoplasm rolling around the nucleus at 2, 8 and 12 min post induction (Fig. 1). From 12 min post induction, the replicated DNA separated into 'clumps' in WT. In mutants, DNA reorganised but did not individualize into distinguishable clumps, even

at 15 min post induction. At these times, the overall cell shape differed between mutant and WT parasites. Δ*Pbkin8B* male gametocytes remained rounded, whereas WT gametocytes started exflagellating. Protrusions labelled with the anti α-tubulin II antibody and corresponding to male gametes could be seen in WT cells, but not in Δ*Pbkin8B* mutants. Even after 30 min post induction, only few exflagellations were recorded in mutants (Suppl. Fig. 2) and no male gamete release was observed by IFA.

WT and Δ*Pbkin8B* male gametocytes were examined by electron microscopy to further examine the effects of the mutation. At 15 min post induction, WT male gametocytes appeared spherical in shape and exhibited an enlarged nucleus in which multiple nuclear poles could be identified, while the cytoplasm containing a number of axonemes (Fig. 2a). Frequently, an electron dense basal body was associated with the nuclear pole and gave rise to an axoneme (Fig. 2b). In cross section, a number, but not all, of the axonemes showed the characteristic 9+2 microtubular organisation (Fig. 2c). In contrast, while a number of mutant male gametocytes appeared spherical (Fig. 2d), others appeared more flattened (data not shown). When examined at higher magnification, the cytoplasm was seen to contain large numbers of elongated, randomly orientated doublet and single microtubules (Fig. 2e). There was no evidence of any coordination of the microtubules to form 9+2 axonemes. In addition, there appeared to be fewer nuclear poles and basal bodies present in the mutant parasites.

Altogether, Δ*Pbkin8B* male gametocytes presented phenotypic characteristics of impaired axoneme formation and male gamete exflagellation, resulting in rounded male cells as previously reported [26, 27].

### 3.2. Global relative quantitative comparative analysis between Δ*Pbkin8B* and WT parasites through gametogenesis

We performed an iTRAQ-based, quantitative and comparative, proteomic analysis of Δ*Pbkin8B* line against the previous WT *P. berghei* analysis [21], performed in parallel during the time-course of the xanthurenic acid-induced gamete development (Fig. 3). From our finding using iTRAQ labelling-based proteomic approach, 530 proteins from 3,198 peptides (FDR < 0.5%) were identified in Δ*Pbkin8B* mutants over the three time points (Suppl. Table S1). Furthermore, 462 mouse blood proteins were identified from 1,344 peptides (Suppl. Table S2).

For WT parasites, considering that 443 proteins were identified over the three time points in the same condition as previously reported [21], the WT and the Δ*Pbkin8B* lines shared 382 proteins (Fig. 4A) corresponding to 86% and 72% of the total of WT and Δ*Pbkin8B* parasite proteins, respectively (Suppl. Table S3). In our experimental conditions, proteins only found in one parasite line, named here Δ*Pbkin8B*-detected and WT-detected proteins (as in the other line, either the expression level was too low to be detected or the protein was not expressed through the gametogenesis) were GO-categorized (Fig. 4B and corresponding proteins in Suppl. Table S3). Most Δ*Pbkin8B*-detected proteins and WT-detected proteins are listed in several processes related to biosynthesis of DNA, RNA and proteins, showing an important differential regulation of acid nucleic and protein synthesis between WT and Δ*Pbkin8B* lines (Fig. 4B). Surprisingly, no protein found in a single parasite line was classified in energy-producing metabolism processes, in particular glycolysis.

*Proteins only found in WT parasite line*

Several WT-detected proteins were assigned as microtubule dynamic-dependant processes: microtubule-based movement, cellular component and chromatin assembly/disassembly, and as DNA packaging (Fig. 4B; Suppl. Table S3).

Among proteins belonging to microtubule-based movement, we highlight kinesin-8B (PBANKA_020270), the object of our study, confirming the gene disruption, kinesin-13 (PBANKA_145830), the dynein heavy chain (PBANKA_092540) of the axoneme outer dynein arm [23] and the subunit 2 of the dynactin complex (PBANKA_135890). Kinesin-8B and -13 were found previously in male gametocytes and gametes, and may play a role in mitosis and/or flagellar regulation [23]. Dyneins are widely conserved and identified in the eukaryotic flagellum. Dynactin subunit 2 is a constituent of the dynactin complex, which modulates cytoplasmic dynein binding to an organelle or anchoring microtubules to chromosomes.

Nucleosome proteins, histone H2B.Z (PBANKA_142060), two histone 3 variants (PBANKA_010880 and PBANKA_111710), and the unknown protein PBANKA_103880 with a EGF-like domain, clustered in chromosome assembly/DNA packaging, have not been found in Δ*Pbkin8B* parasites.

As well as chromatin regulation, the abundance of some motility microtubule-based and structural-based proteins are thus affected in Δ*Pbkin8B* parasites at the proteome level.

*Proteins only found in ΔPbkin8B line*

More than half of the Δ*Pbkin8B*-detected proteins were assigned to metabolic processes related to nucleic acid, amino acid and proteins, indicating an abnormally high level of protein biosynthesis compared to WT parasites. In addition, several were assigned to specific processes: ubiquitin-dependent protein catabolic process (some of them involved in cellular protein modification process as well), organelle organisation process, DNA replication and mismatch repair (Fig. 4B; Suppl. Table S3).

Abnormal or short-lived proteins are targeted for degradation by the proteasome via the posttranslational modification ubiquitination. *P. falciparum* 26S proteasome components and a bacteria-like proteasome are involved in protein degradation [36]. The Δ*Pbkin8B*-specific proteins: AAA-ATPase subunit RPT3 (PBANKA_071560), the regulatory subunits RPT1 (PBANKA_141000), RPN7 (PBANKA_091900) and RPN11 (PBANKA_114400), which are functionally linked, belonging to the 26S proteasome in which the majority of selective cellular protein proteolysis takes place. The ubiquitin carboxyl-terminal hydrolase 2 (PBANKA_123150) might deubiquitinate polyubiquitinated target proteins. The calcyclin-binding protein (PBANKA_145260, PBANKA_083400) might be involved in calcium-dependent ubiquitination and subsequent proteasomal degradation of target proteins. The two proteasome subunits alpha type-6 (PBANKA_122310) and beta type-7 (PBANKA_134330) contribute for a complete assembly of 20S proteasome subunit of the 26S proteasome. In addition, the ubiquitin-activating enzymes E1 (PBANKA_144070) and E2 (PBANKA_060280, PBANKA_010500), and the ubiquitin-conjugating enzyme (PBANKA_113260) were classified in this process.

Some Δ*Pbkin8B*-detected proteins in the organelle organisation process are microtubule-associated proteins, such as dynein light chain 1 (PBANKA_142940) of the axoneme inner dynein arm [23], the dynein intermediate chain (PBANKA_082290), the armadillo repeat protein PF16 (PBANKA_091740), centrin (PBANKA_080060), the MAATS1 domain containing protein (PBANKA_142070), the SOC3 protein (PBANKA_130450) and the radial spoke head protein 9 (RSPH9) homolog (PBANKA_143150). In human patients with primary ciliary dyskinesia, a common mutation

in the radial spoke head protein-encoding gene *RSPH9* gives rise to cilia dysmotility associated with central-microtubular-pair abnormalities [37]. In *Chlamydomonas,* flagella of mutants deficient in entire radial spokes or spoke heads are paralyzed [38]. PF16 was shown to be a key component for the assembly of the central apparatus of *P. berghei* axoneme [39]. Dynein light chain 1 and RSPH9 are structural proteins found inside the axoneme, known to play a role in the mechanical movement of the flagellum/cilium. Regulation of motile 9+2 cilia and flagella depend on interactions between radial spokes and a central pair apparatus. When having improper inner arm and radial spoke organization, flagellum/cilium organisms show a high risk of motile flagella/cilia abnormalities [40].

Other Δ*Pbkin8B*-detected proteins are listed as chromosome-associated, such as histone H4 (PBANKA_094190) and an uncharacterized protein (PBANKA_071600) which is a homolog of the structural maintenance of chromosome protein 3 (SMC-3), a component of the cohesin complex of eukaryotes that is required for sister chromatid cohesion during mitosis and meiosis [41]. In parallel, Δ*Pbkin8B* parasite triggered the synthesis of DNA topoisomerase 2 (PBANKA_101140) that regulates DNA supercoiling and separates interlocked chromosomes, and of DNA replication licensing factor MCM7 (PBANKA_080310), A1 subunit of the replication protein A complex (PBANKA_041660 and 100720) and the replication factor C (PBANKA_031470). *P. falciparum* minichromosome maintenance complex (MCM) plays a key role in the transition of pre-replication complex (before DNA synthesis) to the replication complex [42]. The overexpression of MCM7 subunit has been reported in various premalignant dysplastic lesions and cancers. In *Plasmodium* its expression is up-regulated during the DNA replication of the intraerythrocytic cycle [43]. Finally, DNA mismatch repair protein MSH2 (PBANKA_080430) is involved in the system for repairing damage that can occur during DNA replication and recombination.

### 3.3. Time-specific comparison of Δ*Pbkin8B* and WT regulated proteins through gametogenesis

Protein relative quantification was obtained through iTRAQ labelled peptides for each cell line, and samples were analysed in biological triplicate. There were 59 differentially regulated proteins from Δ*Pbkin8B* parasites at three-time points during differentiation (T0; T7; T15), examining the three intervals T0-T7, T7-T15 and T0-T15. Compared to the 49

differentially regulated proteins from WT parasites [21], both parasite lines shared 31 regulated proteins during gametogenesis (Fig. 5A). Twenty-eight and eighteen proteins were restrictedly modulated in Δ*Pbkin8B* and WT parasites, respectively (Fig. 5B; Suppl. Table S4). These proteins are mainly related to RNA translation and protein biosynthesis, cellular homeostasis and energetic metabolism (Suppl. Table S4). Nonetheless, some line-specific modulated proteins are categorised in cell processes related to the mutant phenotype (Fig. 5B). For example, WT-specific modulated proteins are related to cell motility/ cytoskeleton organization (profilin, PBANKA_083300), cell differentiation/ reproduction (nascent polypeptide associated complex alpha chain, PBANKA_112070). One Δ*Pbkin8B*-specific modulated protein is related to chromosome organization (histone H2A, PBANKA_111700). It should be noted that for the shared proteins, regulation could be reversed (up or down) according to the parasite line. These differences in the expression modulation throughout the cell differentiation, reflect the global disorganisation produced in the mutant line compared to WT.

From a time-dependant pairwise quantitative and comparative analysis at each time T0, and T7 and T15 post induction, the 37 proteins that displayed a difference of abundance between Δ*Pbkin8B* and WT parasites over times of differentiation can be clustered in 6 main important cell processes: host cell haemoglobin degradation and proteolysis, energy metabolism, cytoskeleton and cell motility, nucleic acid and protein synthesis, host interaction and egress, stress and protein folding (Table 1 and Suppl. Table S5).

The most severely affected processes were nucleic acid and protein synthesis, stress and protein folding. The high HSP abundance fluctuation observed among development times evidences that Δ*Pbkin8B* parasites are responding to unfavourable/abnormal developmental conditions.

Concerning the energy metabolism process, globally, the Δ*Pbkin8B* parasites produced less glycolysis enzymes than the WT parasites that would impair the ATP production (Table 1 and Suppl. Table S5).

Δ*Pbkin8B* parasites have a strong deregulation of the most dynamic component of the cytoskeleton and axoneme, the microtubules. Alpha tubulin I (PBANKA_041770) and II (PBANKA_052270) were highly up-regulated in Δ*Pbkin8B* parasites and to the contrary, tubulin beta chain (PBANKA_120690) was down-regulated. The modulation of the 3 proteins

was striking at T7, while Alpha tubulins and beta tubulin showed an increased expression during the gametogenesis of WT parasites [21].

Moreover, two proteins, male development gene 1 (MDV1, PBANKA_143220) and osmiophilic body protein (G377, PBANKA_146300) important for the RBC egress during gametogenesis were found to be up-regulated in the Δ*Pbkin8B* parasites at each time point. To egress, the gametocytes must lyse the two external membrane barriers, the parasitophorous vacuole membrane produced by the parasite and the RBC membrane. The sequential inside-out lysis occurs in response to the exocytosis of specialized secretory vesicles only present in the gametocyte including the osmiophilic bodies [44].

## 4. DISCUSSION

The kinesin-8 family of motors is thought to mediate chromosome movements through a combination of translocation and microtubule depolymerisation activities in budding yeast (Kip3 protein) [20, 45] and human cells (Kif18 protein) [46, 47]. For instance, human Kif18 is involved in regulating the process of chromosome alignment, referred to chromosome congression and considered to be essential for cell viability. Depletion of Kif18A affects kinetochore movements and results in mitotic cells with abnormally long mitotic spindles that fail to congress chromosomes at the metaphase plate. Kif18 is not essential for the establishment and/or maintenance of kinetochore-microtubule attachment but is required for judging tension across kinetochore pairs. Recently, the two kinesin-8, Klp5 and Klp6, in the fission yeast were shown to contribute on microtubule dynamics, kinetochore attachment stability and sliding force in the mitotic spindle [14]. In addition to aberrant chromosome pushing movements, occasional cells lacking Klp5 contained three spindle pole bodies and tripolar mitotic spindles. It was observed that the absence of kinesin-8 in organisms causes cellular polarity defect and longer mitotic spindles but that is not always the case [14, 15]. In the amoeba *Dictyostelium discoideum*, for example, kinesin-8 kif10 is not essential for development or viability and appears to cooperate with dynein to organize the interphase radial microtubule array [14]. This is relevant because *D. discoideum* possesses 13 kinesin-8 isoforms that suggests a functional redundancy of motor isoforms in this organism. Moreover, the variability in reported roles of kinesin-8 members suggest that their effects may be different in different organisms [14].

In *P. berghei*, gene disruption for one of the two kinesin-8 members, PbKIN8B, known to be expressed during male gametogenesis by proteome data [22], caused a main phenotype: a defect in the axoneme assembly affecting the male gamete morphogenesis, the exflagellation process and consequently fertilization [26, 27]. Intranuclear mitoses appeared to be less affected. Ultrastructural analysis revealed a failure in axoneme assembly in Δ*Pbkin8B*: elongated microtubules were seen in longitudinal sections but the classical 9+2 axoneme organisation was never observed. PbKIN8B did not co-localise with kinetochores in the nucleus rather with the cytoplasmic basal bodies and the assembling axoneme during the gametogenesis process, revealing an unexpected role for PbKIN8B in parasite flagellum formation [26, 27]. Several non-exclusive hypotheses for the role of PbKIN8B in flagellum formation were proposed. The absence of PbKIN8B could cause: 1) defects of the basal body and a subsequent abnormal axoneme construction; 2) instability of the assembled axoneme due to disruption of the connections between the axoneme components. On the other hand, an indirect role of PbKIN8B by interacting with specific partners involved in the flagellum formation could not be excluded.

To better understand the role of PbKIN8B in *P. berghei* male gametogenesis, we undertook a quantitative and comparative proteomic analysis between Δ*Pbkin8B* and WT parasites during the course of xanthurenic acid-induced gamete development. Our study shows that Δ*Pbkin8B* gametocyte is metabolically active up to the last time observed, 15 min post induction. However very distinct metabolic and cell physiological states were observed compared to WT parasites at the proteome level. The major proteomic disturbances observed in Δ*Pbkin8B* compared to WT parasites are:

1) A high abundance of proteins involved in ubiquitin-dependent protein catabolic processes such as 26S proteasome subunits and enzymes regulating the protein post-translational modification ubiquitination, concomitant with a high abundance of ribosomal proteins and aminoacyl-tRNA biosynthesis compared to WT parasites. That indicates an abnormal high level of expression of proteins in Δ*Pbkin8B* parasites compared to WT parasites that need to be controlled through a targeted proteolysis via ubiquitination to maintain the cell homeostasis.

2) An unexpected absence of kinesin-13 and a high variation in the abundance of microtubule-associated proteins: no detectable dynein heavy chain of the axoneme outer dynein arm and dynactin subunit 2, and in contrast, an abnormal high abundance of the dynein light chain I, dynein intermediate chain, PF16, centrin, MAATS1 protein, SOC3 protein, and

RSPH9. These proteins play essential roles in the microtubule/axoneme structure and function. Their absence or high abundance correlate with the disrupted axoneme assembly and flagellum formation observed in Δ*Pbkin8B* parasites and support the essential role of PbKIN8B in the axoneme assembly [26, 27]. Flagella formation in *Plasmodium* is unique among the single-celled eukaryotes. They arise from *de novo* formed basal bodies and assemble in the cytoplasm without transport of materials by an intraflagellar transport mechanism as observed in many other organisms. PbKIN8B localises with the basal bodies and the assembling axoneme prior to flagellum formation. Although, a partial loss of the tight association between the basal body and the nuclear pole and a reduced number of basal bodies were reported in the absence of PbKIN8B [26, 27], its particular roles in axoneme assembling stay unsolved. Could the absence of PbKIN8B cause defect at the level of the basal body and in consequence, a perturbation in the axoneme construction? Could PbKIN8B transport essential elements for the axoneme assembly and stability, its absence leading to incomplete constructed or disorganized axonemes?

Previous comparative transcriptional analysis of Δ*Pbkin8B* and WT parasites suggested that the observed mutant phenotype resulted directly from the absence of PbKIN8B rather than through the indirect effect of another protein [27]. Interestingly, we recorded a co-concomitant loss of detection of kinesin-13 and other motor proteins assigned to microtubule-based movement (the dynein heavy chain, the subunit 2 of the dynactin complex) in Δ*Pbkin8B* parasites, suggesting that the regulation is at the protein level. PbKIN13 is one of the three kinesins identified in the male gametocytes and gametes and is localized along the axoneme [48]. Its role in gametogenesis is unknown since PbKIN13 is essential to asexual parasite development [49] that prevents production of *Pbkin13* gene-deleted parasites. Kinesins-13 regulate microtubule dynamics acting as unique depolymerases in that they do not move along microtubules but target microtubule ends to induce disassembly [50]. They are implicated in the mitotic spindle regulation but also in the flagellar length control in a variety of organisms [51]. The absence of PbKIN13 certainly participates in the observed Δ*Pbkin8B* parasite phenotype, as the absence of the heavy chain of the axoneme outer dynein arm that should have, as a consequence, the destabilization of the axoneme structure. One scenario could be that PbKIN8B interactions with axonemal proteins along with several motor proteins (such as dynein and PbKIN13) are essential for their interaction or integration with the growing axoneme. Absence of PbKIN8B results in abnormalities within the axoneme

organisation and leads to a dislocation of the structure as observed by electron microscopy. Non-integrated axonemal proteins are further ubiquitinated and degraded by proteasomes.

3) Besides microtubule-associated proteins, high differences of expression level of proteins involved in chromatin regulation, DNA replication and mismatch repair were observed (proteins not detectable or high abundant in Δ*Pbkin8B* compared to WT parasites). PbKIN8B was not localized in the gametocyte nucleus, nor associated with the mitotic spindles, in contrast with another kinesin-8 family member PbKIN8X [52]. Δ*Pbkin8B* male gametocytes show apparent normal rounds of endomitosis and DNA replication after male gamete induction. At the electron microscopy level, a similar organization of nuclear poles, mitotic spindles and chromatin condensation was observed in Δ*Pbkin8B* and WT induced-gametocytes [26, 27]. Although we observed fewer nuclear poles and basal bodies in the mutant line, that suggested apparent normal first endomitoses occurring in ΔPbkin8B parasites, proteomic data suggested that DNA processes were affected. The way chromatin is organized inside the nucleus of eukaryotic cells is a key factor in gene control and chromosomal organization and dynamics, as well as gene positioning, could influence spatiotemporally gene expression in bacteria [53] and in Eukaryotes [54, 55] and in *Plasmodium* [56]. The link with the absence of PbKIN8B still needs to be deciphered.

4) Amongst common proteins present in Δ*Pbkin8B* and WT parasites, modulation of the expression of some occurs during the course of male gamete formation. They cover important cell processes: host cell haemoglobin degradation and proteolysis, energy metabolism, cytoskeleton and cell motility, nucleic acid and protein synthesis, host interaction and egress, stress and protein folding. These expression modulations throughout male gametogenesis reflect the global disorganisation produced in the mutant line compared to WT.

In summary, PbKIN8B plays an essential role in axoneme assembly during male gamete formation that is essential for parasite transmission to the mosquito. PbKIN8B is associated with the basal body and emerging axoneme. Our proteomic analysis shows that the absence of PbKIN8B results in the absence or in the abnormal high abundance of microtubule- or axonemal-associated proteins that are essential for axoneme organization and stability. This dysregulation explains the major failure in axoneme assembly observed in Δ*Pbkin8B* parasites and suggests an essential role of PbKIN8B for the correct interaction or integration of axonemal proteins within the growing axoneme. This dysregulation is supported by an unusual high expression of proteins involved in the protein biogenesis and the ubiquitin-dependant proteasome proteolysis. Dysregulation of proteins involved in

chromatin organisation and DNA processes was also observed in Δ*Pbkin8B* parasites although DNA condensation, mitotic spindle formation and endomitoses seem to occur. PbKIN8B was not localized in the nucleus and mitotic spindles. The link between PbKIN8B and DNA processes remains to be clarified.

**Figure captions**

**Figure 1.** IFA of WT and Δ*Pbkin8B* during the male gametogenesis at 2, 8, 12 and 15 min post induction by xanthurenic acid. Immunofluorescence images correspond to the maximum intensity projection of the z-series. IFAs were performed using anti-alpha-tubulin II antibody. DNA parasite was revealed using DAPI. Scale bars represent 2 µm.

**Figure 2.** Electron micrographs of WT (a-c) and Δ*Pbkin8B* (d-e) male gametocytes at 15 min post induction of gamete production. Bars represent 1 µm (a, d) and 100 nm on all others. (a) Later stage WT male gametocyte showing the nucleus with multiple (4) nuclear poles (arrows) and a number of longitudinal running axonemes (A). (b) Detail showing a nuclear pole (NP) with associated basal body (B) and axoneme (A). (c) Enlargement showing a cross sectioned axoneme (A) exhibiting the classical 9+2 microtubular arrangement. (d) Mutant male gametocyte containing a central nucleus (N) exhibiting a single nuclear pole (NP), while the cytoplasm contains a number of elongated longitudinally sectioned microtubules (Mt). (e) Detail of the peripheral cytoplasm showing numerous randomly distributed of doublet and single microtubules (Mt).

**Figure 3.** Experimental design and setup for comparative proteomic analysis. WT and Δ*Pbkin8B P. berghei* gametocyte-infected RBC were harvested from mice (1), gametocytes were enriched by NycoDenz density gradient (2), exflagellation trigged by xanthurenic acid (3) and then sampled at 3 time points: 0 min, 7 min and 15 min. For each time point collected, the parasites were lysed in 8 M urea (4) and then proteins subjected to tryptic digestion (5). The resulted peptides were labelled by iTRAQ reagent resulting in multiplexes (6). iTRAQ-labelled peptides were subjected to LC-MS/MS analysis (7). Spectra were interpreted by mass spectrometry software (8).

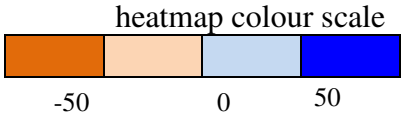
**Figure 4**. Comparison of total identified proteins detected in WT and Δ*Pbkin8B* parasites during the gametogenesis. Venn sets of shared proteins between both lines (A) and the GO categories of proteins found only in each line (B). Process categories correspond to the 148 proteins exclusively detected in Δ*Pbkin8B* mutants in red and to the 61 proteins exclusively detected in WT parasites in blue.

**Figure 5.** Comparison of regulated proteins displayed in WT and Δ*Pbkin8B* parasites during gametogenesis. Venn set of regulated proteins in each line (A) and GO categorization of the proteins regulated (B) in each line. Process categories correspond to the 28 proteins restrictedly modulated in Δ*Pbkin8B* mutants in red and the 18 proteins restrictedly modulated in WT parasites in blue.

**Table 1: Abundance variation of proteins through time point comparison.** According to colour scale, abundance variations were represented in a heatmap representation for easy visualization of time point abundance differential variation.

| Cell process | *Plasmodium berghei* ANKA accession number | WT / Δ*Pbkin8B* | | |
|---|---|---|---|---|
| | | T0 | T7 | T15 |
| **Host cell haemoglobin degradation and proteolysis** | PBANKA_144900 \| aspartyl protease, putative \| length=577 | -69% | -101% | 114% |
| | PBANKA_061030 \| polyubiquitin, putative \| length=229 | – | 7% | -23% |
| **Energy metabolism** | PBANKA_111770 \| malate dehydrogenase, putative (MDH) \| length=313 | 63% | -22% | 68% |
| | PBANKA_112560 \| pyruvate kinase, putative \| length=511 | 3% | 5% | 62% |
| | PBANKA_130860 \| fructose-bisphosphate aldolase 2 (ALDO2) \| length=369 | 73% | 10% | 21% |
| | PBANKA_132640 \| glyceraldehyde-3-phosphate dehydrogenase, putative (GAPDH) \| length=337 | 39% | -35% | 1% |
| | PBANKA_121430 \| enolase, putative (ENO) \| length=446 | -14% | 1% | 66% |
| | PBANKA_134010 \| L-lactate dehydrogenase (LDH) \| length=316 | 64% | 6% | 29% |
| | PBANKA_134040 \| oxidoreductase, putative \| length=334 | -28% | 21% | 21% |
| **Cytoskeleton and cell motility** | PBANKA_120690 \| tubulin beta chain, putative \| length=445 | -7% | 52% | 8% |
| | PBANKA_041770 \| alpha tubulin 1 \| length=453 | – | -15% | -35% |
| | PBANKA_052270 \| alpha tubulin 2 \| length=450 | 5% | -30% | 9% |
| **Nucleic acid and protein synthesis** | PBANKA_121770 \| ATP-dependent RNA helicase DDX6 (DOZI) \| length=433 | -90% | – | -62% |
| | PBANKA_020300 \| chromatin assembly factor 1 protein WD40 domain, putative \| length=446 | 37% | -3% | 28% |
| | PBANKA_113330 (or PBANKA_113340) \| elongation factor 1-alpha (EF-1alpha) \| length=443 | 43% | -5% | -9% |
| | PBANKA_131480 \| elongation factor 2, putative \| length=832 | 39% | 93% | 52% |
| | PBANKA_136030 \| DNA/RNA-binding protein Alba 4, putative (ALBA4) \| length=374 | -74% | -1% | – |
| | PBANKA_091800 \| 60S acidic ribosomal protein P0, putative \| length=315 | – | -117% | 2% |
| | PBANKA_114170 \| ubiquitin-60S ribosomal protein L40, putative \| length=128 | – | 7% | -23% |
| | PBANKA_111300 \| purine nucleoside phosphorylase, putative (PNP) \| length=244 | 43% | 14% | – |
| | PBANKA_143920 \| polyadenylate-binding protein, putative (PABP) \| length=834 | -108% | -12% | 6% |
| | PBANKA_061160 \| ribonucleoside-diphosphate reductase, large subunit, putative \| | – | 20% | 4% |

| | | | | |
|---|---|---|---|---|
| | length=847 | | | |
| | PBANKA_101670 \| conserved Plasmodium protein, unknown function \| length=279 | – | -19% | 3% |
| **Host interaction and egress** | PBANKA_146300 \| osmiophilic body protein (G377) \| length=2606 | – | 79% | -107% |
| | PBANKA_143220 \| male development gene 1 (MDV1) \| length=214 | -32% | -59% | -82% |
| **Stress and protein folding** | PBANKA_071190 \| heat shock protein 70 (HSP70) \| length=693 | 18% | 0% | 7% |
| | PBANKA_081890 \| heat shock protein 70, putative \| length=651 | -33% | 54% | -80% |
| | PBANKA_091440 \| heat shock protein 70, putative (UIS24) \| length=663 | – | 30% | -16% |
| | PBANKA_080570 \| heat shock protein 90, putative (HSP90) \| length=720 | 57% | -26% | 72% |
| | PBANKA_111860 \| cell division cycle protein 48 homologue, putative \| length=815 | 42% | -36% | 101% |
| | PBANKA_070280 \| protein disulfide isomerase \| length=482 | – | 39% | -6% |
| | PBANKA_143730 \| endoplasmin, putative (GRP94) \| length=808 | – | 17% | 0% |
| | PBANKA_093840 \| endoplasmic reticulum-resident calcium binding protein, putative \| length=342 | 47% | – | 135% |
| | PBANKA_121650 \| peptidyl-prolyl cis-trans isomerase, putative (CYP19A) \| length=170 | 113% | -47% | 34% |
| | PBANKA_093220 \| peptidyl-prolyl cis-trans isomerase, putative \| length=192 | -74% | -49% | – |
| **Unknown** | PBANKA_082670 \| conserved Plasmodium protein, unknown function \| length=222 | – | -92% | 14% |



**Supplementary Data**

**Suppl. Figure S1.** Generation and analysis of Δ*Pbkin8B* parasites. **A)** Schematic representation of the vector used to disrupt *Pbkin8B* and the genomic loci before and after insertion of the vector to generate the transgenic parasite line Δ*Pbkin8B* by single crossover. The plasmid used contains the dhfr/ts selection cassette. **B)** (From left to right) Correct disruption of the *Pbkin8B* locus, absence of the episome vector, presence of dhfr/ts cassette, and finally integration of the cassette, were analysed by PCR for two clones (lanes 1 and 2) using the primers indicated.

**Suppl. Figure S2.** Genetic approach reveals PbKIN8B is required to male gametocyte exflagellation. For the experiments, infected erythrocyte samples independently obtained from 17 WT infected-mice and 18 Δ*Pbkin8B*-infected mice were analysed. **A)** Gametocyte production. **B)** Male gametocyte per 100 cells. **C)** Quantification of exflagellation centres per 100 male gametocytes in WT and Δ*Pbkin8B* lines at 15 min post induction (10 x 1 $mm^2$ Malassez square). Statistical differences between WT and Δ*Pbkin8B* cells were analysed by Student's t-test (****$p$<0.0001). Graphs represent mean ± standard deviation.

**Suppl. Table S1.** Δ*Pbkin8B* line proteins identified during gametogenesis.

**Suppl. Table S2.** Rodent proteins identified during Δ*Pbkin8B* line gametogenesis.

**Suppl. Table S3.** Proteins from *P. berghei* wild type and Δ*Pbkin8B* lines comparison during gametogenesis.

**Suppl. Table S4.** Regulated proteins from *P. berghei* wild type and Δ*Pbkin8B* lines comparison during gametogenesis.

**Suppl. Table S5.** Time-specific proteins listing.

## Author contributions

The manuscript was written through contributions of all authors. All authors have given approval to the final version of the manuscript.

The authors declare no competing financial interest.


## Funding sources

This work was supported by CAPES/COFECUB programme [723/11 and 923/18], CNPq (MCTI/CNPq/FNDCT/PRO-CENTRO-OESTE [407730/2013-3 and 407855/2013-0], INCT-MCTI/CNPq/FAPs [16/2014], Universal [430610/2016-5]), CAPES-PROEX, FAPDF [Demanda Espontânea 193.001.723/2017], Finep [CT-Infra grants 0439/11 and 0694/13]. This project was also funded by ATM from Muséum National d'Histoire Naturelle, Paris.

## Acknowledgements

We thank Nuno Domingues, Marlon D. M. Santos, Alan Ribeiro Mol, Dr. Jaques M. F. Souza, Dr. Rayner M. L. Queiroz, and Prof. Wagner Fontes for technical assistance; Joy Alonso for animal cares; Lisy Raveendran and Cyril Willig (CeMIM Platform of the MNHN).


## Abbreviations

CLB, coelenterazine loading buffer; HSP, heat shock protein; ip, intraperitoneally; IFA, immunofluorescence assay; Δ*Pbkin8B,* disrupted *Plasmodium berghei kinesin-8B* gene; PbKIN8B, *Plasmodium berghei* kinesin-8B; RBC, red blood cell; RPMI medium, Roswell Park Memorial Institute medium; TCA, tricarboxylic acid pathway; TEAB, triethylammonium bicarbonate; TFA, trifluoroacetic acid; WT, wild- type.

**References**


[1] WHO, World malaria report 2019, Geneva, 2019.

[2] E.L. Flannery, A.K. Chatterjee, E.A. Winzeler, Antimalarial drug discovery - approaches and progress towards new medicines, Nat Rev Microbiol 11(12) (2013) 849-62.

[3] G.A. Josling, M. Llinas, Sexual development in Plasmodium parasites: knowing when it's time to commit, Nat Rev Microbiol 13(9) (2015) 573-87.

[4] M. Arevalo-Herrera, Y. Solarte, C. Marin, M. Santos, J. Castellanos, J.C. Beier, S.H. Valencia, Malaria transmission blocking immunity and sexual stage vaccines for interrupting malaria transmission in Latin America, Mem Inst Oswaldo Cruz 106 Suppl 1 (2011) 202-11.

[5] D.S. Guttery, A.A. Holder, R. Tewari, Sexual development in Plasmodium: lessons from functional analyses, PLoS Pathog 8(1) (2012) e1002404.

[6] R.E. Sinden, R. Carter, C. Drakeley, D. Leroy, The biology of sexual development of Plasmodium: the design and implementation of transmission-blocking strategies, Malar J 11 (2012) 70.

[7] N. Gerald, B. Mahajan, S. Kumar, Mitosis in the human malaria parasite Plasmodium falciparum, Eukaryot Cell 10(4) (2011) 474-82.

[8] J.R. Kardon, R.D. Vale, Regulators of the cytoplasmic dynein motor, Nat Rev Mol Cell Biol 10(12) (2009) 854-65.

[9] B. Wickstead, K. Gull, A "holistic" kinesin phylogeny reveals new kinesin families and predicts protein functions, Mol Biol Cell 17(4) (2006) 1734-43.

[10] L.A. Fox, K.E. Sawin, W.S. Sale, Kinesin-related proteins in eukaryotic flagella, J Cell Sci 107 ( Pt 6) (1994) 1545-50.

[11] R. Yokoyama, E. O'Toole, S. Ghosh, D.R. Mitchell, Regulation of flagellar dynein activity by a central pair kinesin, Proc Natl Acad Sci U S A 101(50) (2004) 17398-403.

[12] J.T. Kevenaar, S. Bianchi, M. van Spronsen, N. Olieric, J. Lipka, C.P. Frias, M. Mikhaylova, M. Harterink, N. Keijzer, P.S. Wulf, M. Hilbert, L.C. Kapitein, E. de Graaff, A. Ahkmanova, M.O. Steinmetz, C.C. Hoogenraad, Kinesin-Binding Protein Controls Microtubule Dynamics and Cargo Trafficking by Regulating Kinesin Motor Activity, Curr Biol 26(7) (2016) 849-61.

[13] N. Hirokawa, Y. Noda, Intracellular transport and kinesin superfamily proteins, KIFs: structure, function, and dynamics, Physiol Rev 88(3) (2008) 1089-118.

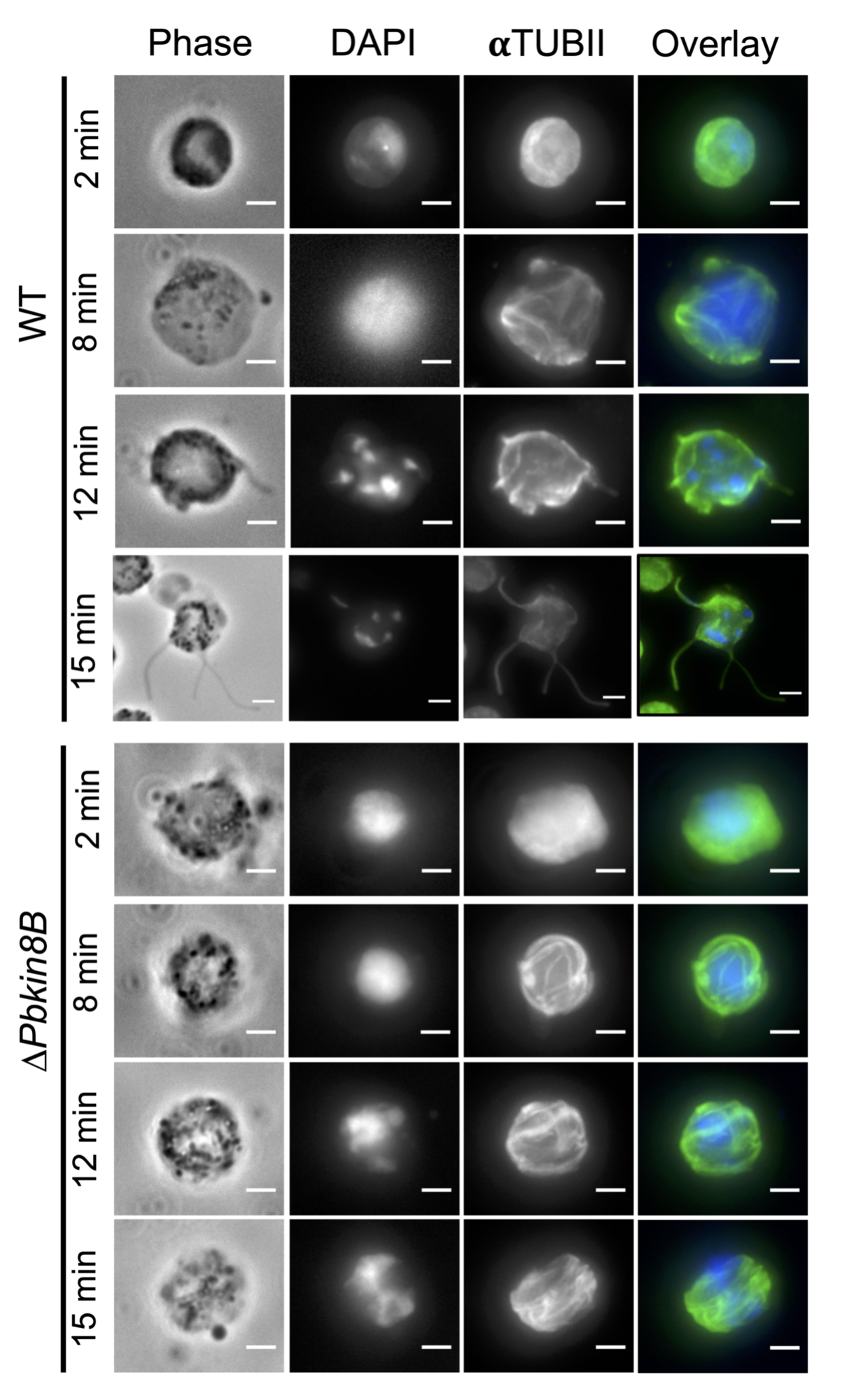
[14] Z.R. Gergely, A. Crapo, L.E. Hough, J.R. McIntosh, M.D. Betterton, Kinesin-8 effects on mitotic microtubule dynamics contribute to spindle function in fission yeast, Mol Biol Cell (2016).
[15] L.J. Messin, J.B. Millar, Role and regulation of kinesin-8 motors through the cell cycle, Syst Synth Biol 8(3) (2014) 205-13.
[16] K.A. Johnson, J.L. Rosenbaum, Polarity of flagellar assembly in Chlamydomonas, J Cell Biol 119(6) (1992) 1605-11.
[17] C.J. Lawrence, R.K. Dawe, K.R. Christie, D.W. Cleveland, S.C. Dawson, S.A. Endow, L.S. Goldstein, H.V. Goodson, N. Hirokawa, J. Howard, R.L. Malmberg, J.R. McIntosh, H. Miki, T.J. Mitchison, Y. Okada, A.S. Reddy, W.M. Saxton, M. Schliwa, J.M. Scholey, R.D. Vale, C.E. Walczak, L. Wordeman, A standardized kinesin nomenclature, J Cell Biol 167(1) (2004) 19-22.
[18] E.J. Tomei, S.M. Wolniak, Transcriptome analysis reveals a diverse family of kinesins essential for spermatogenesis in the fern Marsilea, Cytoskeleton (Hoboken) 73(3) (2016) 145-59.
[19] Y. Shin, Y. Du, S.E. Collier, M.D. Ohi, M.J. Lang, R. Ohi, Biased Brownian motion as a mechanism to facilitate nanometer-scale exploration of the microtubule plus end by a kinesin-8, Proc Natl Acad Sci U S A 112(29) (2015) E3826-35.
[20] M.L. Gupta, Jr., P. Carvalho, D.M. Roof, D. Pellman, Plus end-specific depolymerase activity of Kip3, a kinesin-8 protein, explains its role in positioning the yeast mitotic spindle, Nat Cell Biol 8(9) (2006) 913-23.
[21] C.H.S. Garcia, D. Depoix, R.M.L. Queiroz, J.M.F. Souza, W. Fontes, M.V. de Sousa, M.D.M. Santos, P.C. Carvalho, P. Grellier, S. Charneau, Dynamic molecular events associated to Plasmodium berghei gametogenesis through proteomic approach, J Proteomics 180 (2018) 88-98.
[22] S.M. Khan, B. Franke-Fayard, G.R. Mair, E. Lasonder, C.J. Janse, M. Mann, A.P. Waters, Proteome analysis of separated male and female gametocytes reveals novel sex-specific Plasmodium biology, Cell 121(5) (2005) 675-87.
[23] A.M. Talman, J.H. Prieto, S. Marques, C. Ubaida-Mohien, M. Lawniczak, M.N. Wass, T. Xu, R. Frank, A. Ecker, R.S. Stanway, S. Krishna, M.J. Sternberg, G.K. Christophides, D.R. Graham, R.R. Dinglasan, J.R. Yates, 3rd, R.E. Sinden, Proteomic analysis of the Plasmodium male gamete reveals the key role for glycolysis in flagellar motility, Malar J 13 (2014) 315.

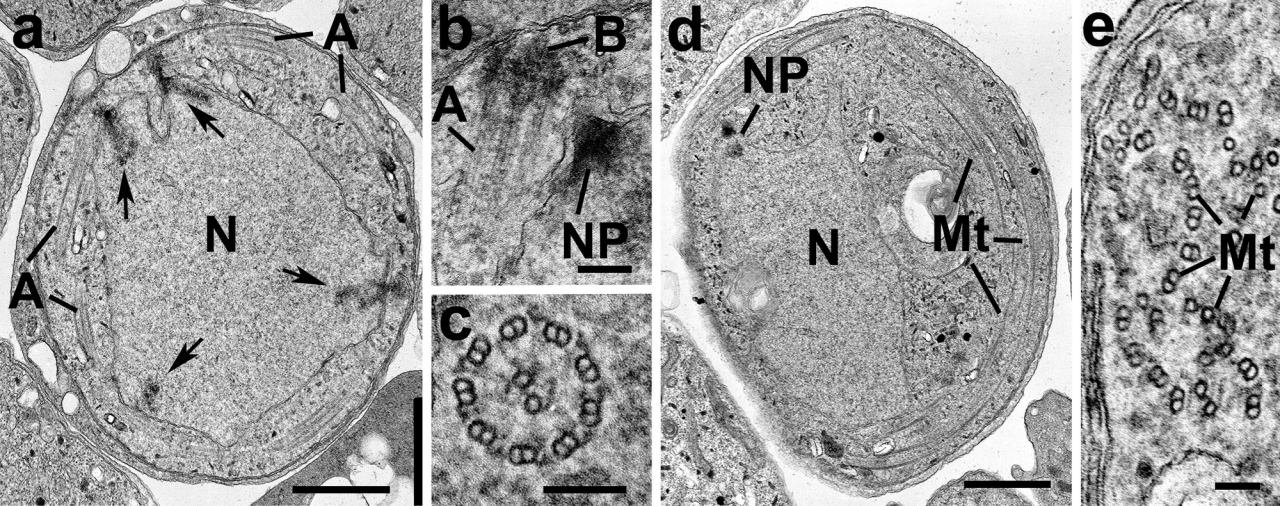
[24] B.M. Invergo, M. Brochet, L. Yu, J. Choudhary, P. Beltrao, O. Billker, Sub-minute Phosphoregulation of Cell Cycle Systems during Plasmodium Gamete Formation, Cell Rep 21(7) (2017) 2017-2029.
[25] R.E. Sinden, The cell biology of malaria infection of mosquito: advances and opportunities, Cellular Microbiology 17(4) (2015) 451-466.
[26] D. Depoix, S.R. Marques, D.J. Ferguson, S. Chaouch, T. Duguet, R.E. Sinden, P. Grellier, L. Kohl, Vital role for Plasmodium berghei Kinesin8B in axoneme assembly during male gamete formation and mosquito transmission, Cell Microbiol 22(3) (2020) e13121.
[27] M. Zeeshan, D.J. Ferguson, S. Abel, A. Burrrell, E. Rea, D. Brady, E. Daniel, M. Delves, S. Vaughan, A.A. Holder, K.G. Le Roch, C.A. Moores, R. Tewari, Kinesin-8B controls basal body function and flagellum formation and is key to malaria transmission, Life Sci Alliance 2(4) (2019).
[28] T.F. de Koning-Ward, A.W. Thomas, A.P. Waters, C.J. Janse, Stable expression of green fluorescent protein in blood and mosquito stages of Plasmodium berghei, Mol Biochem Parasitol 97(1-2) (1998) 247-52.
[29] C.J. Janse, J. Ramesar, A.P. Waters, High-efficiency transfection and drug selection of genetically transformed blood stages of the rodent malaria parasite Plasmodium berghei, Nat Protoc 1(1) (2006) 346-56.
[30] A.L. Beetsma, T.J. van de Wiel, R.W. Sauerwein, W.M. Eling, Plasmodium berghei ANKA: purification of large numbers of infectious gametocytes, Exp Parasitol 88(1) (1998) 69-72.
[31] D.S. Guttery, D.J. Ferguson, B. Poulin, Z. Xu, U. Straschil, O. Klop, L. Solyakov, S.M. Sandrini, D. Brady, C.A. Nieduszynski, C.J. Janse, A.A. Holder, A.B. Tobin, R. Tewari, A putative homologue of CDC20/CDH1 in the malaria parasite is essential for male gamete development, PLoS Pathog 8(2) (2012) e1002554.
[32] L.M.A. Flanagan J. P., Controlled phenylhydrazine-induced reticulocytosis in the rat, The Ohio journal of science 70(5) (1970) 5.
[33] J. Gobom, E. Nordhoff, E. Mirgorodskaya, R. Ekman, P. Roepstorff, Sample purification and preparation technique based on nano-scale reversed-phase columns for the sensitive analysis of complex peptide mixtures by matrix-assisted laser desorption/ionization mass spectrometry, J Mass Spectrom 34(2) (1999) 105-16.
[34] Y. Perez-Riverol, A. Csordas, J. Bai, M. Bernal-Llinares, S. Hewapathirana, D.J. Kundu, A. Inuganti, J. Griss, G. Mayer, M. Eisenacher, E. Pérez, J. Uszkoreit, J. Pfeuffer, T. Sachsenberg, S. Yilmaz, S. Tiwary, J. Cox, E. Audain, M. Walzer, A.F. Jarnuczak, T.

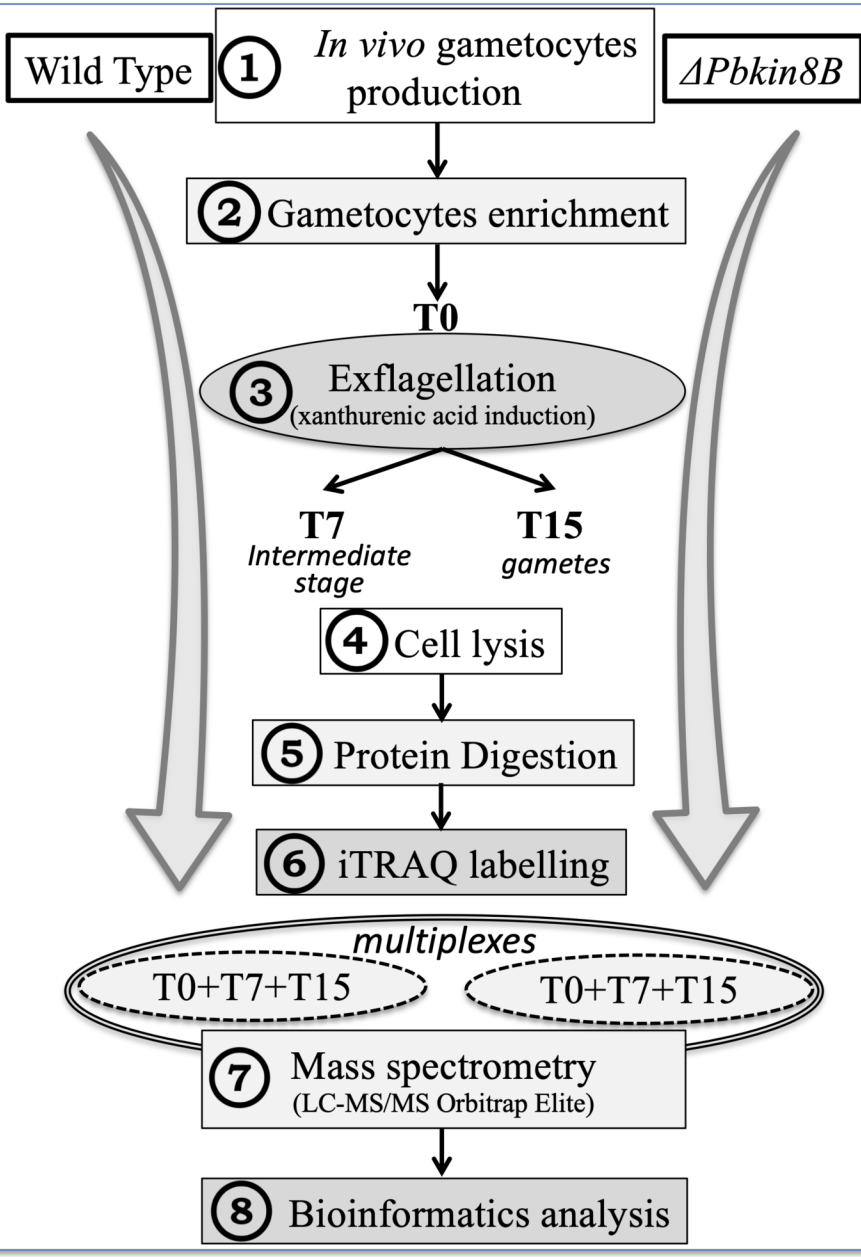
Ternent, A. Brazma, J.A. Vizcaíno, The PRIDE database and related tools and resources in 2019: improving support for quantification data, Nucleic Acids Res 47(D1) (2019) D442-D450.
[35] P.C. Carvalho, D.B. Lima, F.V. Leprevost, M.D. Santos, J.S. Fischer, P.F. Aquino, J.J. Moresco, J.R. Yates, 3rd, V.C. Barbosa, Integrated analysis of shotgun proteomic data with PatternLab for proteomics 4.0, Nat Protoc 11(1) (2016) 102-17.
[36] D.W. Chung, N. Ponts, J. Prudhomme, E.M. Rodrigues, K.G. Le Roch, Characterization of the ubiquitylating components of the human malaria parasite's protein degradation pathway, PLoS One 7(8) (2012) e43477.
[37] O. Reish, M. Slatkin, D. Chapman-Shimshoni, A. Elizur, B. Chioza, V. Castleman, H.M. Mitchison, Founder mutation(s) in the RSPH9 gene leading to primary ciliary dyskinesia in two inbred Bedouin families, Ann Hum Genet 74(2) (2010) 117-25.
[38] D. White, S. Aghigh, I. Magder, J. Cosson, P. Huitorel, C. Gagnon, Two anti-radial spoke monoclonal antibodies inhibit Chlamydomonas axonemal motility by different mechanisms, J Biol Chem 280(15) (2005) 14803-10.
[39] U. Straschil, A.M. Talman, D.J. Ferguson, K.A. Bunting, Z. Xu, E. Bailes, R.E. Sinden, A.A. Holder, E.F. Smith, J.C. Coates, Rita Tewari, The Armadillo repeat protein PF16 is essential for flagellar structure and function in Plasmodium male gametes, PLoS One 5(9) (2010) e12901.
[40] J. Lin, T. Heuser, B.I. Carbajal-González, K. Song, D. Nicastro, The structural heterogeneity of radial spokes in cilia and flagella is conserved, Cytoskeleton (Hoboken) 69(2) (2012) 88-100.
[41] T. Hirano, At the heart of the chromosome: SMC proteins in action, Nat Rev Mol Cell Biol 7(5) (2006) 311-22.
[42] S. Patterson, C. Robert, C. Whittle, R. Chakrabarti, C. Doerig, D. Chakrabarti, Pre-replication complex organization in the atypical DNA replication cycle of Plasmodium falciparum: characterization of the mini-chromosome maintenance (MCM) complex formation, Mol Biochem Parasitol 145(1) (2006) 50-9.
[43] A. Ansari, R. Tuteja, Genome wide comparative comprehensive analysis of Plasmodium falciparum MCM family with human host, Commun Integr Biol 5(6) (2012) 607-15.
[44] J. Kehrer, F. Frischknecht, G.R. Mair, Proteomic Analysis of the Plasmodium berghei Gametocyte Egressome and Vesicular bioID of Osmiophilic Body Proteins Identifies Merozoite TRAP-like Protein (MTRAP) as an Essential Factor for Parasite Transmission, Mol Cell Proteomics 15(9) (2016) 2852-62.

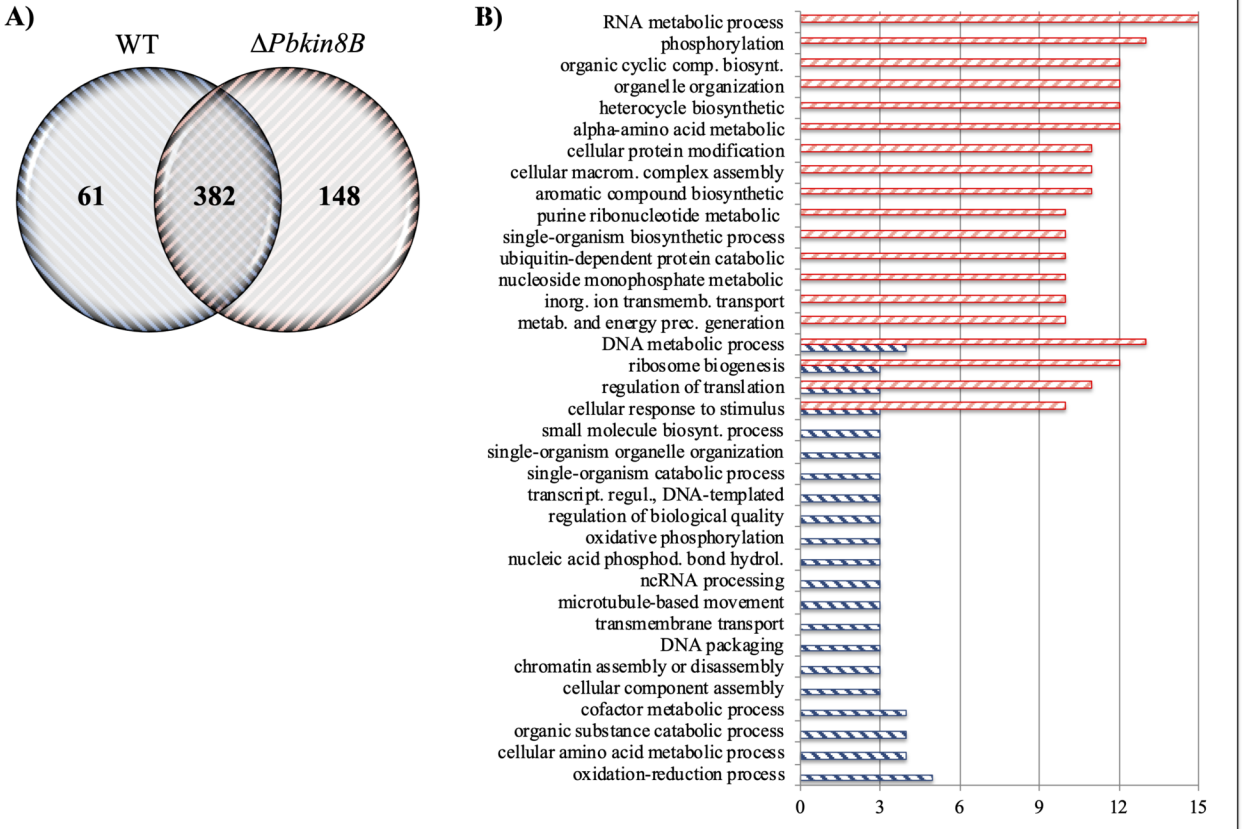
[45] V. Varga, J. Helenius, K. Tanaka, A.A. Hyman, T.U. Tanaka, J. Howard, Yeast kinesin-8 depolymerizes microtubules in a length-dependent manner, Nat Cell Biol 8(9) (2006) 957-62.
[46] J. Stumpff, L. Wordeman, Chromosome congression: the kinesin-8-step path to alignment, Curr Biol 17(9) (2007) R326-8.
[47] C. Zhu, J. Zhao, M. Bibikova, J.D. Leverson, E. Bossy-Wetzel, J.B. Fan, R.T. Abraham, W. Jiang, Functional analysis of human microtubule-based motor proteins, the kinesins and dyneins, in mitosis/cytokinesis using RNA interference, Mol Biol Cell 16(7) (2005) 3187-99.
[48] M.N. Wass, R. Stanway, A.M. Blagborough, K. Lal, J.H. Prieto, D. Raine, M.J. Sternberg, A.M. Talman, F. Tomley, J. Yates, R.E. Sinden, Proteomic analysis of Plasmodium in the mosquito: progress and pitfalls, Parasitology 139(9) (2012) 1131-45.
[49] E. Bushell, A.R. Gomes, T. Sanderson, B. Anar, G. Girling, C. Herd, T. Metcalf, K. Modrzynska, F. Schwach, R.E. Martin, M.W. Mather, G.I. McFadden, L. Parts, G.G. Rutledge, A.B. Vaidya, K. Wengelnik, J.C. Rayner, O. Billker, Functional Profiling of a Plasmodium Genome Reveals an Abundance of Essential Genes, Cell 170(2) (2017) 260-272.e8.
[50] W. Wang, S. Cantos-Fernandes, Y. Lv, H. Kuerban, S. Ahmad, C. Wang, B. Gigant, Insight into microtubule disassembly by kinesin-13s from the structure of Kif2C bound to tubulin, Nat Commun 8(1) (2017) 70.
[51] S.C. Dawson, M.S. Sagolla, J.J. Mancuso, D.J. Woessner, S.A. House, L. Fritz-Laylin, W.Z. Cande, Kinesin-13 regulates flagellar, interphase, and mitotic microtubule dynamics in Giardia intestinalis, Eukaryot Cell 6(12) (2007) 2354-64.
[52] M. Zeeshan, F. Shilliday, T. Liu, S. Abel, T. Mourier, D.J.P. Ferguson, E. Rea, R.R. Stanway, M. Roques, D. Williams, E. Daniel, D. Brady, A.J. Roberts, A.A. Holder, A. Pain, K.G. Le Roch, C.A. Moores, R. Tewari, Plasmodium kinesin-8X associates with mitotic spindles and is essential for oocyst development during parasite proliferation and transmission, PLoS Pathog 15(10) (2019) e1008048.
[53] P. Sobetzko, A. Travers, G. Muskhelishvili, Gene order and chromosome dynamics coordinate spatiotemporal gene expression during the bacterial growth cycle, Proc Natl Acad Sci U S A 109(2) (2012) E42-50.
[54] D.L. Spector, The dynamics of chromosome organization and gene regulation, Annu Rev Biochem 72 (2003) 573-608.
[55] R. Schneider, R. Grosschedl, Dynamics and interplay of nuclear architecture, genome organization, and gene expression, Genes Dev 21(23) (2007) 3027-43.

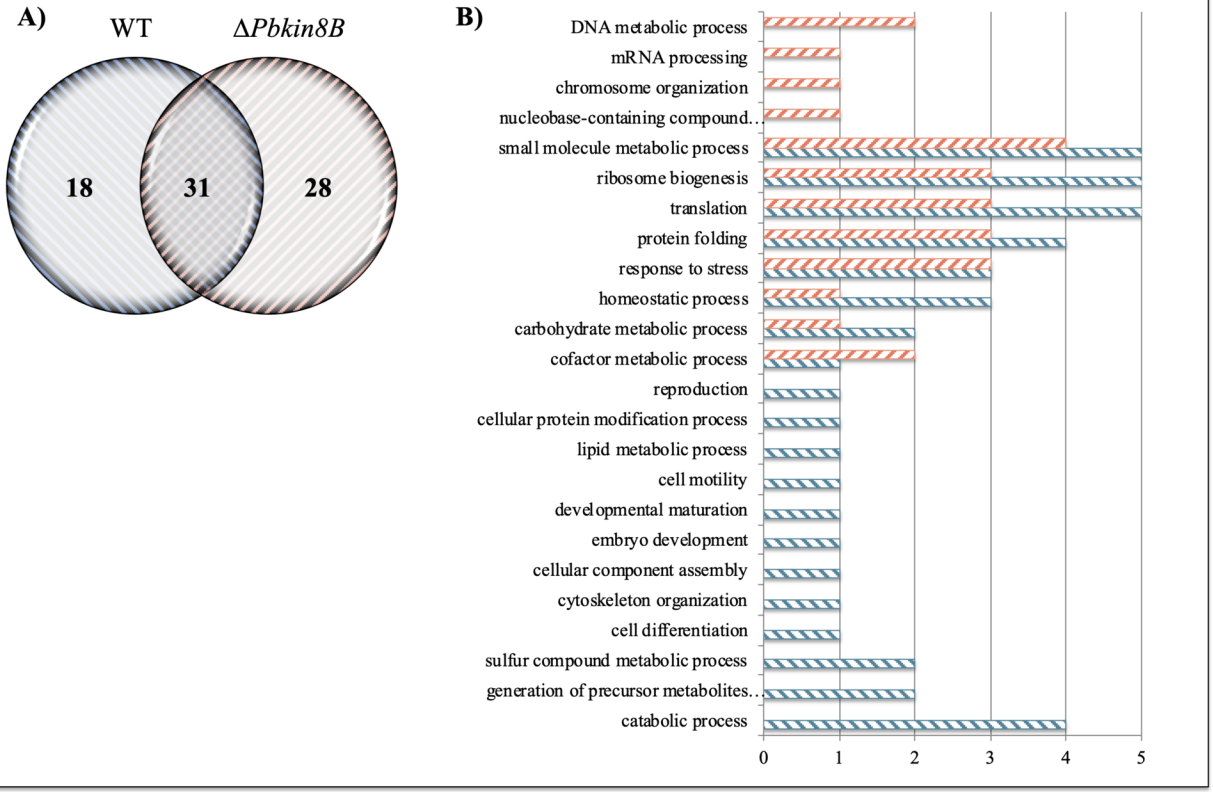
[56] M.F. Duffy, S.A. Selvarajah, G.A. Josling, M. Petter, The role of chromatin in Plasmodium gene expression, Cell Microbiol 14(6) (2012) 819-28.


Phase
DAPI
αTUBII
Overlay
WT
2 min
8 min
12 min
15 min
ΔPbkin8B
2 min
8 min
12 min
15 min

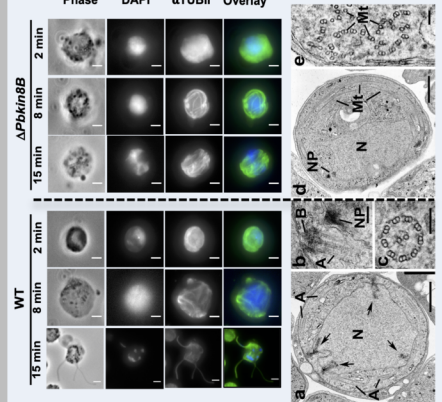

a
A
A
N
b
B
A
NP
c
d
NP
N
Mt
e
Mt


Wild Type
1
In vivo gametocytes production
ΔPbkin8B
2 Gametocytes enrichment
T0
3 Exflagellation
(xanthurenic acid induction)
T7
Intermediate stage
T15
gametes
4 Cell lysis
5 Protein Digestion
6 iTRAQ labelling
multiplexes
T0+T7+T15
T0+T7+T15
7 Mass spectrometry
(LC-MS/MS Orbitrap Elite)
8 Bioinformatics analysis


A)
WT
ΔPbkin8B
61
382
148
B)
RNA metabolic process
phosphorylation
organic cyclic comp. biosynt.
organelle organization
heterocycle biosynthetic
alpha-amino acid metabolic
cellular protein modification
cellular macrom. complex assembly
aromatic compound biosynthetic
purine ribonucleotide metabolic
single-organism biosynthetic process
ubiquitin-dependent protein catabolic
nucleoside monophosphate metabolic
inorg. ion transmemb. transport
metab. and energy prec. generation
DNA metabolic process
ribosome biogenesis
regulation of translation
cellular response to stimulus
small molecule biosynt. process
single-organism organelle organization
single-organism catabolic process
transcript. regul., DNA-templated
regulation of biological quality
oxidative phosphorylation
nucleic acid phosphod. bond hydrol.
ncRNA processing
microtubule-based movement
transmembrane transport
DNA packaging
chromatin assembly or disassembly
cellular component assembly
cofactor metabolic process
organic substance catabolic process
cellular amino acid metabolic process
oxidation-reduction process
0
3
6
9
12
15


A)
WT
ΔPbkin8B
18
31
28
B)
DNA metabolic process
mRNA processing
chromosome organization
nucleobase-containing compound…
small molecule metabolic process
ribosome biogenesis
translation
protein folding
response to stress
homeostatic process
carbohydrate metabolic process
cofactor metabolic process
reproduction
cellular protein modification process
lipid metabolic process
cell motility
developmental maturation
embryo development
cellular component assembly
cytoskeleton organization
cell differentiation
sulfur compound metabolic process
generation of precursor metabolites…
catabolic process
0
1
2
3
4
5

## Phenotypic effects of disruption of kinesin-8B during male gametogenesis




## Proteomic effects of disruption of kinesin-8B during male gamete formation

**Differential expression**

↓ kinesin-13; dynein heavy chain of the axoneme outer dynein arm and dynactin S/U 2

---

↑ dynein light chain I; dynein intermediate chain; PF16; centrin; MAATS1 protein; SOC3 protein and RSPH9

**PbKIN8B plays an essential role in axoneme assembly**